Chemical Engineering Journal 164 (2010) 29–36

Contents lists available at ScienceDirect

Chemical Engineering Journal

journal homepage: www.elsevier.com/locate/cej

A critical study on the adsorption of heterocyclic sulfur and nitrogen compounds by activated carbon: Equilibrium, kinetics and thermodynamics

Jie Wen[a,b], Xue Han[b], Hongfei Lin[b], Ying Zheng[b,*], Wei Chu[a,*]

[a] Department of Chemical Engineering, Sichuan University, Chengdu, China
[b] Department of Chemical Engineering, University of New Brunswick, Fredericton, NB, Canada

ARTICLE INFO

Article history:
Received 24 April 2010
Received in revised form 28 July 2010
Accepted 29 July 2010

Keywords:
Adsorptive removal
Heterocyclic sulfur and nitrogen
Equilibrium
Kinetics
Thermodynamics

ABSTRACT

Adsorption of heterocyclic sulfur and nitrogen compounds by activated carbon was studied using model diesel fuels, light cycle oils and shale oil. It is observed that the carbon favours adsorption of cyclic nitrogen compounds. This work also investigates the equilibrium, kinetics and thermodynamics of adsorption of nitrogen and sulfur compounds from diesel fractions by activated carbon. Quinoline, indole, and carbazole are typical N compounds while dibenzothiophene and 4,6-dimethyldibenzothiophene are the representatives of refractory S compounds in diesel fractions, were selected as the model compounds. The total N adsorbed by the activated carbon is more than the S compound. Comparing the three nitrogen compounds, quinoline shows a greater removal rate than indole and carbazole. Adsorptive removal kinetics for N/S compounds was monitored by a GC-FID (gas chromatograph coupled with flame ionization detector) technique and was found to follow pseudo second-order kinetics. The external diffusion is not a controlling step in the adsorption process. The isotherm indicates that activated carbon presents a highly heterogeneous surface in the adsorption of DBT, quinoline and indole, while a homogeneous surface is observed in the adsorption of carbazole. Negative adsorption free energy suggests that the adsorption process is favourable and spontaneous for all S/N compounds.

1. Introduction

Refineries are facing stringent regulations on the heteroatom contents in their major products such as diesel and gasoline. The sulfur content of diesel fuel must be reduced to be less than 15 ppm [1,2]. At present, deep hydrodesulfurization (HDS) is commercially accomplished by hydrotreating under high temperatures and pressures [3]. The low sulfur content regulated by the new legislation cannot be readily achieved using conventional hydrogenation catalysts and processes [4,5]. Most of the remaining sulfur species after the conventional hydroprocessing treatment are dibenzothiophene (DBT) and its alkyl derivatives. The steric hindrance of substituting groups in the 4,6-position of DBT molecules makes conversion by hydrogenation or hydrogenolysis almost impossible [6,7]. An alternative to hydrodesulfurization (HDS) is adsorptive removal of refractory sulfur compounds from fuels. Adsorption can be performed at ambient temperature and pressure and the content of sulfur in fuels can be reduced to a very low level.

On the other hand, it is also beneficial to remove heterocyclic nitrogen compounds from various refinery streams before (oil is) further processed in subsequent processes, such as isomerization, reforming, catalytic cracking and hydrocracking, where the catalysts are very sensitive to nitrogen compounds. The basic nitrogen compounds can be adsorbed strongly on the acidic sites of various catalysts used in petroleum refining processes, resulting in the poisoning of the active sites [8]. NH_3 produced from denitrogenation reactions is also a poison to the catalysts in the hydrocarbon process [9]. Additionally, the hydrodenitrogenation (HDN) of all heterocyclic nitrogen compounds in gas oil is complicated and has high hydrogen consumptions as N–C cleavage can be accomplished only after its heteroaromatic ring is fully saturated [10]. Again, using adsorbents to pre-remove nitrogen compounds from liquid hydrocarbon fuels is another way to promote hydrodesulfurization (HDS) activity for producing ultra-clean fuels.

Liquid hydrocarbons contain not only the nitrogen and sulfur compounds but also a large amount of structurally similar aromatic compounds [11]. It is a great challenge to identify an adsorbent that can selectively adsorb the nitrogen/sulfur compounds but not coexisting aromatic compounds. Several types of adsorbents have been studied for adsorptive denitrogenation or desulfurization of liquid hydrocarbon fuels, including zeolite [12], activated carbon [13–15], activated alumina [15,16] and silica gel [17]. It was observed that some activated carbons can have much higher adsorption capacities for sulfur and nitrogen compounds than activated alumina and silica gel [11,13,14]. The porous structure and surface chemistry of activated carbons (ACs) was identified as important in the

* Corresponding authors.
E-mail addresses: yzheng@unb.ca (Y. Zheng), chuwei1965@scu.edu.cn (W. Chu).

1385-8947/$ – see front matter © 2010 Elsevier B.V. All rights reserved.
doi:10.1016/j.cej.2010.07.068

Table 1.1
The composition of model fuel, MF#1.

Chemicals	Molar concentration (μmol/g)
S (or N) compound[a]	23.8
Dodecane	Balanced

[a] The S(or N) compound is one of carbazole, quinoline, indole, DBT and 4,6-DMDBT.

adsorption of S and N compounds. Sano et al. [14] reported that the large surface area and the surface oxygen functional group of activated carbon are the key factors in determining the performance of the adsorptive desulfurization and denitrogenation of real gas oil. Zhou et al. [18] evidenced that an increase in surface oxygen groups can facilitate the adsorption capacity of sulfur compounds. Jiang et al. [19] reported that mesopore volume plays an important role in determining the adsorption capacity. However, few attempts have been made in studying the engineering aspects of the process of adsorptive removal of nitrogen/sulfur from liquid hydrocarbons, such as kinetics, isotherm and thermodynamics of the adsorption processes of heterocyclic sulfur and nitrogen. The main objective of this study is to address these aspects with activated carbon used as sorbent material.

2. Experimental

Activated carbon, wood based with H_3PO_4 activation, was purchased from Westvaco and was dried at 120 °C for 24 h before use. A BELSORP-max (Belsorp Japan) was used to determine the physical property of the carbon. The result shows that the activated carbon has a surface area of 2330 m^2/g and micropore volume (*t*-plot) of 1.36 mL/g and the pore sizes ranging 0.6–1 nm. The FTIR spectra of activated carbon were obtained using a Nicolet 6700 FTIR spectrometer within the range of 400–4000 cm^{-1}. Samples of particle size <45 μm were first dried in an oven for 24 h at a temperature of 383 K. The dried samples were mixed with finely divided KBr at a ratio of 1:400.

Adsorption studies were conducted using model diesel fuels, light cycle oils and shale oil. Model diesel fuels contain one or more S/N compounds dissolved in dodecane. Model fuels are designed to simulate diesel fuel. The model diesel fuel contains a single S (or N) compound in dodecane and is denoted as MF#1. The composition of MF#1 is shown in Table 1.1. Dibenzothiophene (DBT) and 4,6-dimethydibenzothiophene (4,6-DMDBT) are used to represent sulfur compounds. Quinoline, indole and carbazole are the model nitrogen compounds. Quinoline is a basic nitrogen while indole and carbazole are neutral nitrogen compounds. MF#2 is the model diesel fuel consisting of both S and N compounds. The concentrations of N and S are shown in Table 1.2. The composition of MF#3 is shown in Table 1.3. MF#3 is similar to MF#2 but contains aromatics. 10 wt.% of ethyl acetate was introduced to MF#3 in order to increase the solubility of carbazole in MF#3. All compounds were obtained from Sigma–Aldrich Co. and used as received. The properties of light cycled oils (LCO) and shale oil are shown in Table 2. All nitrogen compounds in LCO1 and LCO2 are neutral. DBT and its derivatives take approximately 74% and 41%, respectively, of the total sulfur in LCO1 and LCO2. Shale oil contains both basic and neutral nitrogen compounds and the ratio of basic to neutral nitrogen is about 0.09. All sulfur compounds in shale oil are thiophenic sulfur compounds.

Table 1.2
The composition of model fuel, MF#2.

Chemicals	Molar concentration (μmol/g)
Carbazole	23.8
Quinoline	23.8
Indole	23.8
DBT	23.8
Dodecane	Balanced

Table 1.3
The composition of model fuel, MF#3.

Chemicals	Concentration		Molar concentration (μmol/g)
	wt.%	ppmw N/S	
Sulfur compounds			
DBT	0.44	761.6	23.8
Total		761.6	
Nitrogen compounds			
Carbazole	0.42	333.3	23.8
Quinoline	0.31	333.3	23.8
Indole	0.28	333.3	23.8
Total		999.9	
Aromatics			
Naphtalene	0.31		23.8
1-Methylnaphalene	40.00		
Total	40.31		
Paraffin			
Dodecane	Balanced		
Others			
Ethyl acetate	10.00		
Total	100.00		

In batch adsorption, the ratio of activated carbon to model fuel is kept at 1:50 (mass) for all runs. The tests have been carried out in capped vials with continuous stirring at ambient temperature and atmospheric pressure. Adsorption tests were also examined in a fixed-bed flowing system with a glass tubing column and using MF#3 as the feed. 0.5 g of activated carbons, diluted by glass beads of size 20–40 mesh, were packed in the glass tubing column. The two ends of the glass column were filled with glass wool fibers. An HPLC pump was used to provide a liquid flow rate of 0.1 mL/min. The treated model fuel was periodically sampled every 15–20 min, until the saturation point was reached.

For the isotherm study, only one nitrogen or sulfur compound was dissolved in dodecane. The molar concentrations for nitrogen compound were varied at 4.8 μmol/g, 9.5 μmol/g, 14.3 μmol/g, 19.0 μmol/g, 23.8 μmol/g and sulfur compound at 7.9 μmol/g, 15.9 μmol/g, 23.8 μmol/g, 31.7 μmol/g and 39.7 μmol/g. The isotherm tests were conducted at three different temperatures (298 K, 313 K and 328 K) and a water bath was used to maintain the temperature during the adsorption. All the samples generated from model diesel fuels were analyzed by a Varian GC450 gas chromatograph equipped with a capillary column (RTX-5, L:

Table 2
Compositions of light cycle oils and shale oil.

		LCO1	LCO2	Shale oil
Nitrogen	ppmw	520	166	4606
Sulfur	ppmw	5268	14449	375.7
1-Ring aromatics	wt.%	13.8	13.7	–
2-Ring aromatics	wt.%	49.1	56.7	–
Poly-aromatics	wt.%	9.2	5.9	–
SimDist				
% off	Initial boiling point (K)			
5	280/408		265/389	–
10	408/442		389/436	–
30	442/490		436/483	–
50	490/530		483/517	–
70	530/577		517/554	–
90	577/641		554/609	–
95	641/667		609/634	–
EP	732		688	–

Table 3
Adsorption results of real diesel fuels and shale oil.

Feedstock	Concentration ratio of fuels before adsorption	Adsorptive capacity		N selectivity[a]
	S/N	*S* (mmol/mg)	*N* (mmol/mg)	
LCO1	10.2	0.30	0.56	0.65
LCO2	86.8	0.31	0.58	0.65
Shale oil	0.08	0.03	2.40	0.986

[a] N selectivity = the amount of N adsorbed by 1 g carbon/the amount of S and N adsorbed by 1 g carbon.

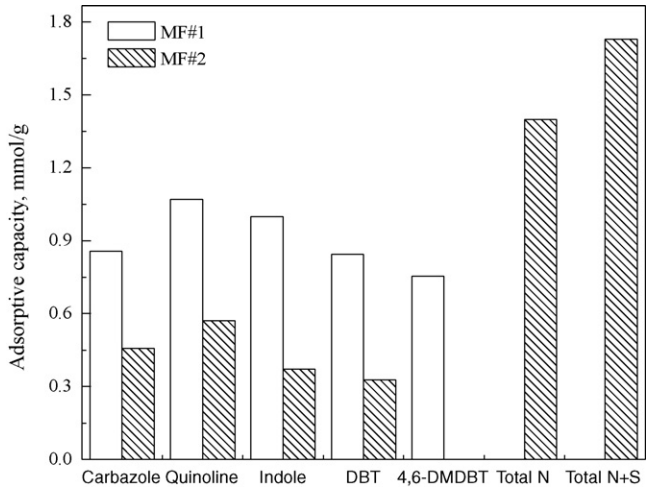

Fig. 1. Adsorptive capacities of activated carbon for different model fuels.

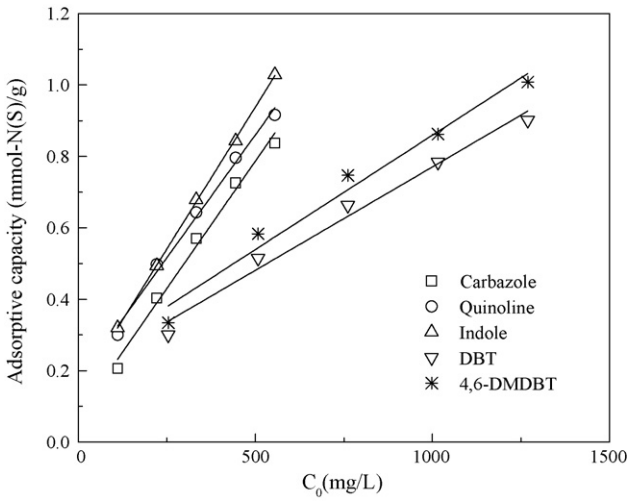

Fig. 2. Effect of initial concentration on equilibrium at 298 K.

15 m, ID: 0.25 mm, DF: 0.25 μm; Restek Corp.) and a flame ionized detector (FID) and a PFPD detector for quantification. The total concentrations of sulfur and nitrogen were analyzed using ANTEK NS-9000.

3. Results and discussion

3.1. Adsorption study

Batch adsorption tests were conducted using two different model fuels, MF#1 and MF#2. The tests were performed overnight. MF#1 contains a single containment component, either one nitrogen compound or one sulfur compound, while MF#2 consists of DBT and three nitrogen compounds. The results are shown in Fig. 1. It is seen that the adsorptive capacities of nitrogen containing compounds are slightly higher than those of sulfur containing compounds. As MF#1 is replaced by MF#2, the total adsorptive capacity for S and N is doubled as a fourfold increase is introduced to the total S and N concentrations of the feed. This observation indicates that the adsorption of N and S compounds is a concentration-driven adsorption, but there is a maximum adsorption capacity for the carbon adsorbent. Concerning each individual S/N compound, it is noted that there is a significant drop in the adsorptive capacity. With model fuel MF#2 as an adsorbate, adsorbed S takes about 19% of the total adsorbed S and N, which is in contrast to 25% of S in the initial molar concentration of total S and N. This seems to suggest that nitrogen compounds compete with sulfur for active sites of activated carbon, and this activated carbon favours adsorbing nitrogen compounds.

Fig. 2 shows the effect of initial concentration, C_0, on the adsorption of S/N onto activated carbon. Model diesel fuel MF#1 with different initial concentrations was examined. The equilibrium adsorption capacity of five different S/N compounds appears to increase linearly with initial concentrations. The three nitrogen compounds have a similar increase rate which is higher than the increase rates of the two sulfur compounds.

MF#3 is used to study the breakthrough curves. Fig. 3 shows the breakthrough curves of various compounds. Naphthalene is a model compound for aromatics. Little naphthalene is absorbed, indicating that this activated carbon has a good selectivity for sulfur and nitrogen compounds. It is also shown that there is no breakthrough point for DBT. This may be because the adsorption rate of DBT is much slower than the adsorption rates of N compounds, which further suggests that this activated carbon favours adsorbing nitrogen compounds.

Three different real feedstocks were studied using the activated carbon. The results are shown in Table 3. For the two light cycle oils, the sulfur content is much higher than the nitrogen con-

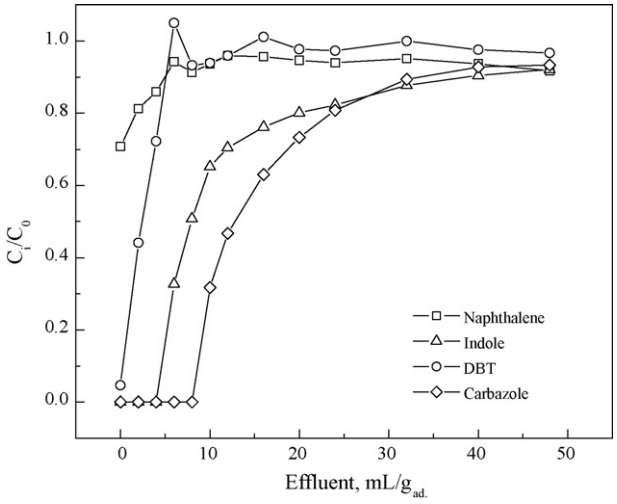

Fig. 3. Breakthrough curves at 298 K.

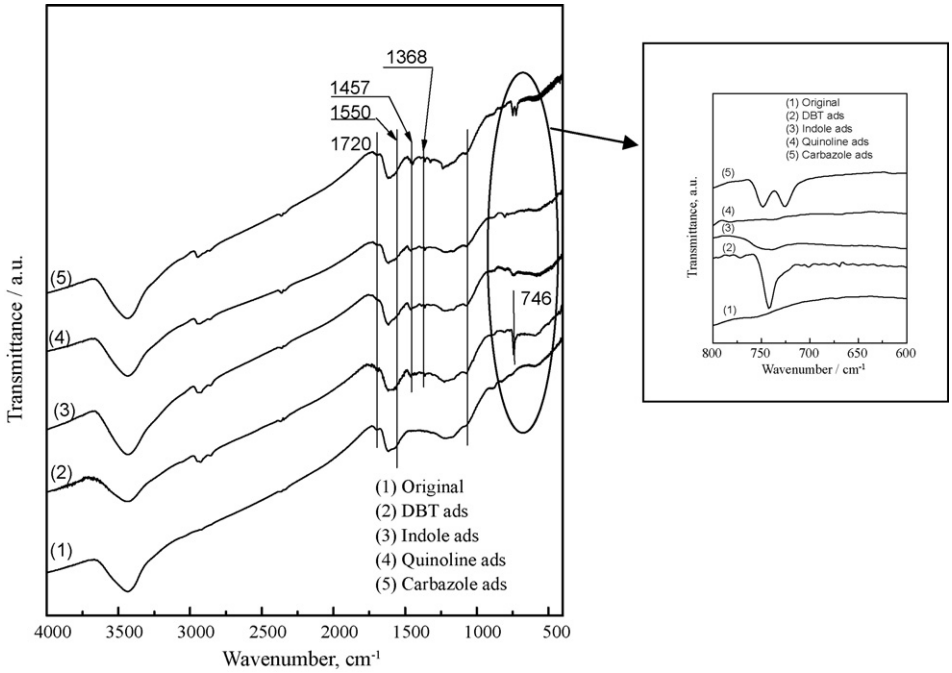

Fig. 4. FTIR spectra of fresh and spent activated carbon.

tent. When the S/N ratio of light cycle oils increases from 10.2 to 86.7, the adsorptive capacities of total sulfur and nitrogen compounds are unchanged, which are 0.3–0.31 mmol-S/mg for sulfur and 0.56–0.58 mmol-N/mg for nitrogen. The nitrogen selectivity is the same for the two light cycle oils, 0.65. This may indicate that with the presence of a significant amount of sulfur compounds in both light cycle oils, all active sites for the adsorption of sulfur have been taken. A further increase in sulfur content in light cycle oil leads to no increase in adsorption capacity for this activated carbon. When shale oil is applied, the adsorptive capacity for total nitrogen compounds is sharply increased up to 2.4 mmol-N/mg, while the adsorptive capacity for total sulfur compounds is reduced to 0.03 mmol-S/mg. The nitrogen selectivity reaches 0.986. This is apparently due to the very low S/N ratio. In consideration of the results presented in Fig. 1 in line with Table 3, one may note that sulfur and nitrogen compounds are adsorbed prominently onto different active sites of the activated carbon. Nitrogen compounds may also take the active sites for the adsorption of sulfur compounds when the concentration of nitrogen is dominant in the feedstock. However, sulfur compounds seem not to have the privilege to take nitrogen sites. A detailed study on the adsorption of types of sulfur and nitrogen compounds may be necessary.

3.2. FTIR analysis

Fig. 4 shows the IR spectra of the fresh activated carbon and the carbons spent in MF#1 with the initial concentration of 23.8 μmol/g for S/N compounds. The absorption bands in the range of 3000–3600 cm^{-1} can be ascribed to the stretching vibration of the hydroxyl groups (O–H) involved in hydrogen bonding and/or water adsorption on the carbons. The new vibrations at 1368 cm^{-1} and between 2950 and 2800 cm^{-1} occurring for spent carbons are due to the asymmetrical stretching of CH_2 and CH_3 from dodecane solvent. The bands in the range of 1850–1350 cm^{-1} are mainly the absorption bands of C=O, C–N– and aromatic rings. The little peak centered at 1720 cm^{-1} shown on both spent and fresh carbons can be a contribution from the stretching vibrations of carboxyl groups (C=O) from activated carbon [18]. The peak at 1550 cm^{-1} may be assigned to asymmetric COO^- vibrations from activated carbon, while 1457 cm^{-1} may be due to C=C of aromatic rings, which is shown only for spent carbons.

It is also noted, from Fig. 4, that a sharp peak at 746 cm^{-1} is formed for the carbon spent with DBT model fuel. This peak may be attributed to the C–S bond in the thiophene ring [20]. In the range of 750–720 cm^{-1}, the characteristic peaks of the carbons spent in carbazole and indole model fuels are different from that of DBT adsorbed carbon. Two sharp peaks at 746 cm^{-1} and 724 cm^{-1}, respectively, can be seen from the spectrum of the carbon spent in carbazole model fuel. These two peaks are attributable to C–H deformation out of the carbazole ring [21,22]. On the other hand, one broad peak at 742 cm^{-1} can be seen for the spectrum of carbon spent in indole model fuel. It is ascribed to the out-of-plane deformation of the C–H bond in the benzene ring, as reported by other researchers [23,24].

Table 4
Langmuir and Freundlich constant values of activated carbon (T = 298 K).

	Langmuir			Freundlich		
	q_m (mmol/g)	K_L (L/mg)	R^2	$1/n$	K_F ($mmol^{1-(1/n)}\ L^{1/n}/g$)	R^2
Carbazole	1.1924	0.0239	0.9983	0.5795	0.0637	0.9813
DBT	1.1236	0.0049	0.9868	0.4628	0.0646	0.9983
Quinoline	1.1774	0.0098	0.9677	0.4507	0.0477	0.9965
Indole	1.3284	0.0092	0.8902	0.4509	0.0755	0.9661

Table 5
Langmuir and Freundlich constant values of activated carbon (T = 313 K).

	Langmuir			Freundlich		
	q_m (mmol/g)	K_L (L/mg)	R^2	$1/n$	K_F (mmol$^{1-(1/n)}$ L$^{1/n}$/g)	R^2
Carbazole	1.1605	0.0229	0.9987	0.5745	0.0615	0.9813
DBT	1.1529	0.0034	0.8935	0.413	0.0545	0.9046
Quinoline	1.1264	0.0093	0.9765	0.4666	0.0594	0.9974
Indole	1.0064	0.0092	0.9143	0.4455	0.0590	0.9151

Table 6
Langmuir and Freundlich constant values of activated carbon (T = 328 K).

	Langmuir			Freundlich		
	q_m (mmol/g)	K_L (L/mg)	R^2	$1/n$	K_F (mmol$^{1-(1/n)}$ L$^{1/n}$/g)	R^2
Carbazole	1.1583	0.021	0.988	0.5773	0.0581	0.9806
DBT	1.5753	0.0015	0.8714	0.6035	0.0155	0.9623
Quinoline	1.1264	0.0074	0.9765	0.5013	0.0457	0.9926
Indole	1.0204	0.0018	0.9067	0.2914	0.1632	0.8124

Table 7
Gibbs free energy for adsorption of S/N onto activated carbon at different temperatures.

T (K)	ΔG^0 (kJ/mol)				K			
	Carbazole	DBT	Quinoline	Indole	Carbazole	DBT	Quinoline	Indole
298	−14.70	−12.59	−11.55	−11.36	377.06	160.85	105.66	98.22
313	−0.007	−0.030	−0.028	−0.037	350.65	86.96	93.05	69.89
328	−0.008	−0.040	−0.034	−0.025	324.49	67.77	79.18	107.3

3.3. Adsorption isotherm

Model fuel MF#1 with different initial concentrations of the S or N species was used to study the adsorption isotherm. The Langmuir and Freundlich isotherm equations have been widely used to analyze equilibrium adsorption data. These mathematical forms of the isotherms are shown as follows:

$$\text{Langmuir isotherm}: \quad q_e = \frac{q_m K_L c_e}{1 + K_L c_e} \tag{1}$$

$$\text{Freundlich isotherm}: \quad q_e = K_F C_e^{1/n} \tag{2}$$

where C_e (mg/L) is the concentration of S/N at equilibrium; K_L (L/mg) and q_m (mmol/g) are the Langmuir constants related to the energy of adsorption and the maximum capacity, respectively; K_F (mmol$^{1-(1/n)}$ L$^{1/n}$/g) and $1/n$ are the Freundlich constants related to the adsorption capacity and intensity, respectively; and q_e (mmol/g) is the molar amount of S/N adsorbed per mass of adsorbent. The linear forms of the Langmuir and Freundlich equations are given by Eqs. (3) and (4).

$$\frac{c_e}{q_e} = \frac{1}{q_m K_L} + \frac{c_e}{q_m} \tag{3}$$

$$\ln\ q_e = \ln K_F + \tfrac{1}{n} \ln C_e \tag{4}$$

The model parameters and the statistical fits of the adsorption data obtained at 298 K to these equations are given in Table 4. The results show that the Langmuir model describes the adsorption of carbazole better than the Freundlich model does, with a correlation factor R^2 value being 0.998. This suggests that the applicability of homogeneous adsorption and the monolayer coverage of carbazole on the surface of activated carbons and the maximum adsorption capacity is 1.2 mmol/g. On the other hand, Freundlich model fits the equilibrium data obtained for DBT, quinoline and indole better than Langmuir model with R^2 values >0.96. The value of $1/n < 1$ generally indicates that adsorption capacity is slightly suppressed at lower equilibrium concentrations. This isotherm indicates activated carbon presents a highly heterogeneous surface in the adsorption of DBT, quinoline and indole. Furthermore, the Freundlich model does not predict saturation adsorption; thus infinite surface coverage is expected to occur, which may lead to a conclusion of multilayer adsorption of DBT, quinoline and indole on the surface of activated carbon [25].

Isotherm parameters for Langmuir and Freundlich isotherms at 313 K and 328 K are given in Tables 5 and 6, respectively. Comparing Table 4 to Tables 5 and 6 will show that the effect of temperature on the adsorption capacity of heterocyclic nitrogen compounds is insignificant. On the contrary, temperature has a pronounced effect on the adsorption of DBT. An increase in temperature from 298 K to 328 K leads to a rise in q_e from ~1.12 mmol-S/g to ~1.58 mmol-S/g. The increase in the adsorption capacity of DBT with an increase in temperature may be attributed to chemisorptions.

The thermodynamic parameters for the adsorption process were calculated using the following expression:

$$\Delta G^0 = -RT \ln\ K \tag{5}$$

The effect of temperature on the equilibrium constant is determined by:

$$\ln\ K = \frac{\Delta S^0}{R} - \frac{\Delta H^0}{RT} \tag{6}$$

The process of adsorption of heterocyclic sulfur or nitrogen compounds represents a reversible process [26].

$$\text{Adsorbate in solution} \Leftrightarrow \text{adsorbate in adsorbent} \tag{7}$$

The apparent equilibrium constant is the ratio of the concentration of adsorbate in adsorbent to the concentration of adsorbate in

Table 8
Enthalpy and entropy for adsorption of S/N onto activated carbon.

	ΔH^0 (kJ/mol)	ΔS^0 (kJ/mol)
Carbazole	−4.06	35.71
DBT	−23.53	−37.22
Quinoline	−7.80	12.65
Indole	2.06	44.03

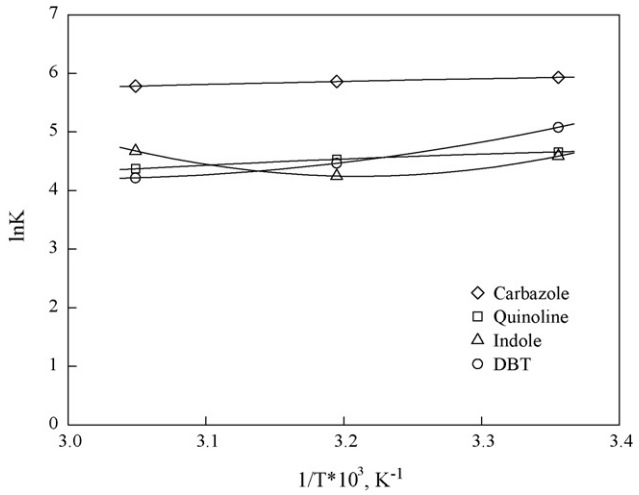

Fig. 5. Relationship between ln K and $1/T$.

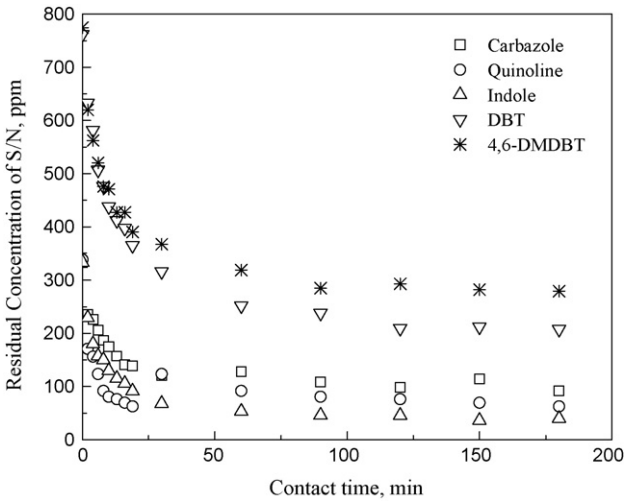

Fig. 6. Effect of contact time on removal of S/N compounds.

solution.

$$K_e = \frac{q_e}{c_e} \tag{8}$$

The thermodynamic equilibrium constant, K, was computed by determining K_e at different initial concentrations of adsorbate and extrapolating to zero. The Gibbs free energy, ΔG^0, for the adsorption process was determined using Eq. (5). The values of K and ΔG^0 for S/N compounds at different temperatures are given in Table 7. The equilibrium constant, K, decreased with increasing temperature for S/N compounds except indole. The overall Gibbs free energy, ΔG^0, is negative for all S/N compounds at the three tested temperatures. ΔG^0 of all tested S/N compounds has a sharp increase as the adsorption temperature increases from 298 K to 313 K and then slightly drops with a further rise in temperature from 313 K to 328 K. Negative adsorption free energy suggests that the adsorption process is favourable and spontaneous for all S/N compounds.

Fig. 5 shows the linear relationship between ln K and $1/T$. The relation of ln K vs. $1/T$ for indole is not linear. ΔH^0 and ΔS^0 can be estimated from the slope and intercept of this linear relationship. The estimated results are shown in Table 8. The enthalpies for carbazole, quinoline and DBT are negative, indicating that the adsorption is favourable at a relatively low temperature, 298 K. The positive enthalpy for indole shows an endothermic process. Indole is not stable and is easy to be oxidized, in particular at a relatively high temperature, 328 K. A light redness was observed at an elevated temperature during the adsorption, which may be responsible for the positive value of enthalpy. Positive entropies for nitrogen components suggest an increased randomness at the solid/solution interface in the adsorption of nitrogen components. On the contrary, the negative adsorption entropy for DBT suggests that the more ordered arrangement of DBT molecules are adsorbed on the surface of activated carbon.

3.4. Adsorption dynamics

Fig. 6 shows the effect of contact time on the batch adsorption of S/N compounds at room temperature and atmospheric pressure. The model oils (MF#1) were kept in contact with the adsorbents for 24 h. The results reveal that the uptake of adsorbate species is fast at the initial stages of the contact period, and thereafter it becomes much slower. Approximately 90% of S/N was removed in the first 3-h contact time. After 3 h of contact time, a steady-state approximation was approaching.

The study of adsorption dynamics describes the adsorbate uptake rate, and evidently this rate controls the residence time of adsorbate uptake at the solid/solution interface. The kinetics of S/N adsorbed onto the activated carbon was analyzed using pseudo first-order and pseudo second-order kinetic models [27]. The pseudo first-order expressed by the Lagergren equation is as follows:

$$\frac{dq_t}{dt} = k_{1ad}(q_e - q_t) \tag{9}$$

where q_e and q_t are the adsorption capacity at equilibrium and at time t, respectively (mmol/g), and k_{1ad} is the rate constant of pseudo first-order adsorption (min^{-1}). After integrating Eq. (9) and applying boundary conditions $t = 0$ to $t = t$ and $q_t = 0$ to $q_t = q_t$ to the integrated form, Eq. (9) becomes:

$$\log(q_e - q_t) = \log\ q_e - \frac{k_{1ad}t}{2.303} \tag{10}$$

The values of $\log(q_e - q_t)$ were linearly correlated with t. The plot of $\log(q_e - q_t)$ vs. t should give a linear relationship from which k_{1ad} can be determined from the slope of the plot.

The pseudo second-order adsorption kinetic rate equation is expressed by Eq. (11):

$$\frac{dq_t}{dt} = k_{2ad}(q_e - q_t)^2 \tag{11}$$

where k_{2ad} is the rate constant of pseudo second-order adsorption (mmol/mg/min). With the boundary conditions $t = 0$ to $t = t$ and $q_t = 0$ to $q_t = q_t$, integrate Eq. (11) and rearrange the integrated form to obtain Eq. (12).

$$\frac{t}{q_t} = \frac{1}{k_{2ad}q_e^2} + \frac{t}{q_e} \tag{12}$$

and

$$h = k_{2ad}q_e^2 \tag{13}$$

h is the initial adsorption rate at time approaching $t = 0$ (mmol/g/min). The plot of (t/q_t) and t of Eq. (12) should give a linear relationship from which k_{2ad} can be determined from the intercept of the plot. The results of fitting experimental data with the pseudo first-order and pseudo second-order models for the adsorption of S/N compounds onto activated carbon are presented in Table 9. As can be seen, the correlation coefficients (R^2) are 0.98–0.99 for the pseudo second-order model and 0.91–0.94

Table 9
Adsorption kinetic models rate constants for different S and N compounds.

Adsorbates	Pseudo first-order		Pseudo second-order			
	Rate constants k_{1ad} (min^{-1})	R^2	Rate constants k_{2ad} (mmol/g/min)	R^2	h	q_e[a]
Carbazole	0.0721	0.9485	0.2641	0.9824	0.1908	0.8500
Indole	0.0700	0.9217	0.2672	0.9963	0.2733	1.0113
Quinoline	0.1253	0.9163	0.4168	0.9965	0.5005	1.0958
DBT	0.0492	0.9400	0.1753	0.992	0.1217	0.8333
4,6-DMDBT	0.0751	0.9434	0.3021	0.9918	0.1578	0.7228

[a] Calculated by pseudo second-order model.

for the pseudo first-order model. This indicates that the adsorption of S and N compounds onto activated carbon follows pseudo second-order kinetics. Quinoline has a larger constant k_{2ad} and a higher initial adsorption rate h than the other two nitrogen components. This may be attributable to the fact that quinoline is a basic nitrogen and contains lone pair electrons, which introduces a significant dipole moment resulting in attractive forces.

The S/N compounds transport from the liquid phase of model oil to the surface of activated carbon takes several steps. The overall adsorption process may be controlled by either one or more steps: external diffusion, pore diffusion, and adsorption on the sorbent surface [28,29]. The possibility of intra-particle diffusion on adsorption was explored by Weber and Morris model [30].

$$q_t = k_{id} t^{1/2} + C \quad (14)$$

Fig. 7 shows the Weber–Morris plot of q_t vs. $t^{0.5}$ for S and N compounds. Apparently, there are two linear zones (zone 1 and zone 2) exhibiting for the adsorption process, which indicates that more than one step of adsorption resistances dominate in the uptake of S/N by activated carbon. For the three N compounds, the initial linear zone ends at $t^{0.5} = 4\ min^{1/2}$, earlier than that in sulfur adsorption process, whose initial linear zone ends at about $8\ min^{1/2}$. The initial linear zone describes external surface adsorption where the adsorbate diffuses from the liquid phase to the external surface of the adsorbent. The second linear zone refers to the gradual adsorption stage and the final equilibrium stage in which the intra-particle diffusion dominates.

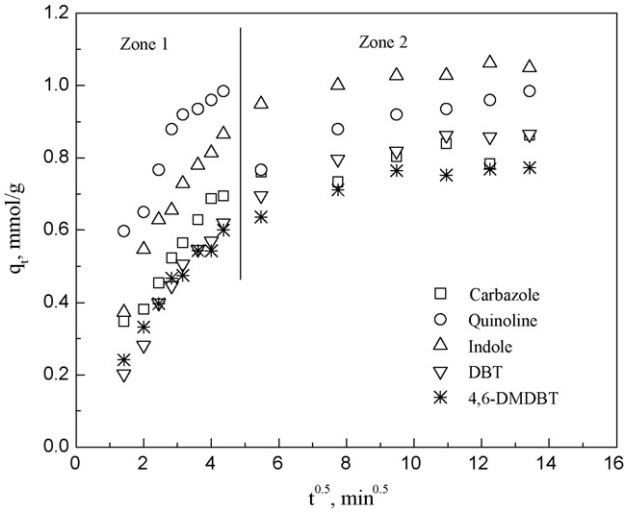

Fig. 7. Weber and Morris intra-particle diffusion plot for the adsorption of S/N by activated carbon.

4. Conclusion

In this study, for the first time, the engineering aspects of the process of the adsorptive removal of nitrogen/sulfur compounds were studied. The following results were obtained:

(1). Model diesel fuels, light cycle oils and shale oil have been used to study the adsorption by activated carbon. This activated carbon favours adsorbing nitrogen compounds. Sulfur and nitrogen seem to be adsorbed on different active sites.
(2). The isotherm results indicate that the activated carbon presents a highly heterogeneous surface in the adsorption of DBT, quinoline and indole, while it presents a homogeneous surface in the adsorption of carbazole. Negative adsorption free energies are obtained for all tested S/N compounds, which suggests that the adsorption process is favourable and spontaneous. The increase in the adsorption capacity of DBT with an increase in temperature may be attributed to chemisorptions. Positive entropies for nitrogen components suggest an increased randomness at the solid/solution interface in the adsorption of nitrogen components.
(3). The adsorption of S and N compounds onto activated carbon follows pseudo second-order kinetics. For all the S/N compounds studied, the external diffusion is not a controlling step in the adsorption process, while the intra-particle diffusion dominates the adsorption process. Quinoline shows a faster adsorption rate than the other two nitrogen components do.

Acknowledgements

The authors are grateful for the financial support provided by the Atlantic Innovation Fund and Imperial Oil.

References

[1] News-EPA, Government developments-EPA, Oil Gas J. 1 (2001) 7.
[2] C.S. Song, An overview of new approaches to deep desulfurization for ultra-clean gasoline, Catal. Today 86 (2003) 211–263.
[3] M. Breysse, G. Djega-Mariadassou, S. Pessayre, C. Geantet, M. Vrinat, G. Perot, M. Lemaire, Deep desulfurization: reactions, catalysts and technological challenges, Catal. Today 84 (3–4) (2003) 129–138.
[4] L.H. Ding, Z.S. Zhang, Y. Zheng, Z. Ring, J.W. Chen, Effect of fluorine and boron modification on the HDS, HDN and HDA activity of hydrotreating catalysts, Appl. Catal. A 301 (2006) 241–250.
[5] L.H. Ding, Y. Zheng, Z.S. Zhang, Z. Ring, J.W. Chen, Hydrotreating of light cycled oil using WNi/Al_2O_3 catalysts containing zeolite beta and/or chemically treated zeolite Y, J. Catal. 241 (2006) 435–445.
[6] V. Meille, E. Schulz, M. Lemaire, M. Vrinat, Hydrodesulfurization of alkyldibenzothiophenes over a $NiMo/Al_2O_3$ catalyst: kinetics and mechanism, J. Catal. 170 (1997) 29–36.
[7] F. Bataille, J.L. Lemberton, P. Michaud, G. Pérot, M. Vrinat, M. Lemaire, E. Schulz, M. Breysse, S. Kasztelan, Alkyldibenzothiophenes hydrodesulfurization-promoter effect, reactivity, and reaction mechanism, J. Catal. 191 (2000) 409–422.
[8] K. Liu, F.T.T. Ng, Effect of the nitrogen heterocyclic compounds on hydrodesulfurization using in situ hydrogen and a dispersed Mo catalyst, Catal. Today 149 (2010) 28–34.
[9] E. Furimsky, Hydrodenitrogenation of petroleum, Cat. Rev. Sci. Eng. 47 (2005) 297–489.

[10] S. Eijsbouts, V.H.J. Debeer, R. Prins, Hydrodenitrogenation of quinoline over carbon-supported transition-metal sulphides, J. Catal. 127 (1991) 619–630.
[11] J.H. Kim, X.L. Ma, A.N. Zhou, C.S. Song, Ultra-deep desulfurization and denitrogenation of diesel fuel by selective adsorption over three different adsorbents: a study on adsorptive selectivity and mechanism, Catal. Today 111 (2006) 74–83.
[12] A.J. Hernandez-Maldonado, R.T. Yang, Denitrogenation of transportation fuels by zeolites at ambient temperature and pressure, Angew. Chem. Int. Ed. 43 (2004) 1004–1006.
[13] Y. Sano, K.H. Choi, Y. Korai, I. Mochida, Adsorptive removal of sulfur and nitrogen species from a straight run gas oil over activated carbons for its deep hydrodesulfurization, Appl. Catal. B 49 (2004) 219–225.
[14] Y. Sano, K.H. Choi, Y. Korai, I. Mochida, Selection and further activation of activated carbons for removal of nitrogen species in gas oil as a pretreatment for its deep hydrodesulfurization, Energy Fuel 18 (2004) 644–651.
[15] M. Almarri, X.L. Ma, C.S. Song, Selective adsorption for removal of nitrogen compounds from liquid hydrocarbon streams over carbon- and alumina-based adsorbents, Ind. Eng. Chem. Res. 48 (2009) 951–960.
[16] A. Srivastav, V.C. Srivastava, Adsorptive desulfurization by activated alumina, J. Hazard. Mater. 170 (2009) 1133–1140.
[17] K.H. Choi, Y. Korai, I. Mochida, J.W. Ryu, W. Min, Impact of removal extent of nitrogen species in gas oil on its HDS performance: an efficient approach to its ultra deep desulfurization, Appl. Catal. B 50 (2004) 9–16.
[18] A.N. Zhou, X.L. Ma, C.S. Song, Effects of oxidative modification of carbon surface on the adsorption of sulfur compounds in diesel fuel, Appl. Catal. B 87 (2009) 190–199.
[19] Z.X. Jiang, Y. Liu, X.P. Sun, F.P. Tian, F.X. Sun, C.H. Liang, W.S. You, C.R. Han, C. Li, Activated carbons chemically modified by concentrated H_2SO_4 for the adsorption of the pollutants from wastewater and the dibenzothiophene from fuel oils, Langmuir 19 (2003) 731–736.
[20] K. Castillo, J.G. Parsons, D. Chavez, et al., Oxidation of dibenzothiophene to dibenzothiophene-sulfone using silica gel, J. Catal. 2 (2009) 329–334.
[21] M. Tamada, H. Koshikawa, H. Omichi, Real-time in situ observation of PVD of N-vinylcarbazole with FTIR-RAS, Thin Solid Films 1–2 (1997) 113–116.
[22] W.J. Lao, C.Z. Xu, S.F. Ji, et al., Electronic and vibrational spectra of a series of substituted carbazole derivatives, Spectrochim. Acta A 11 (2000) 2049–2060.
[23] H. Talbi, E.B. Maarouf, B. Humbert, et al., Spectroscopic studies of electrochemically doped polyindole, J. Phys. Chem. Solids 6–8 (1996) 1145–1151.
[24] F. Wan, L. Liang, X.B. Wan, et al., Modification of polyindole by the incorporation of pyrrole unit, J. Appl. Polym. Sci. 4 (2002) 814–820.
[25] D. Nibou, H. Mekatel, S. Amokrane, M. Barkat, M. Trari, Adsorption of Zn^{2+} ions onto NaA and NaX zeolites: Kinetic, equilibrium and thermodynamic studies, J. Hazard. Mater. 173 (2010) 637–646.
[26] A.K. Bhattacharya, T.K. Naiya, S.N. Mandal, S.K. Das, Adsorption, kinetics and equilibrium studies on removal of Cr(VI) from aqueous solutions using different low-cost adsorbents, Chem. Eng. J. 137 (2008) 529–541.
[27] D.M. Ruthven, Principles of Adsorption and Adsorption Process, John Wiley, New York, 1984.
[28] V. Vimonses, S.M. Lei, B. Jin, C.W.K. Chowd, C. Saint, Kinetic study and equilibrium isotherm analysis of Congo Red Adsorption by clay materials, Chem. Eng. J. 148 (2009) 354–364.
[29] M. Alkan, O. Demirbas, S. Celikcapa, M. Dogan, Sorption of Acid Red 57 from aqueous solution onto sepiolite, J. Hazard. Mater. 116 (2004) 135–145.
[30] W.J. Weber, J.C. Morris, Kinetics of adsorption on carbon solution, J. Sanit. Eng. Div. ASCE 89 (1963) 31–60.